Selective Syntheses of Homo- and Hetero-dimetal Complexes with the Tetramethyltetraazaannulene Ligand of the Type [(ML,M′L′)(TMTAA)], Where M and M′ Are Rh(I) or Ir(I) and L and L′ Are COD or $(CO)_2$

Rosa Fandos,[†,‡] Marc D. Walter,[†] Daniel Kazhdan,[†] and Richard A. Andersen*[,†]

Department of Chemistry and Chemical Sciences Division of Lawrence Berkeley National Laboratory, University of California, Berkeley, California 94720, and Facultad de Ciencias del Medio Ambiente, Universidad de Castilla−La Mancha, 45071 Toledo, Spain

Received January 12, 2006

The tetraazamacrocycle, tmtaaH_2, reacts with [M_2(COD)$_2$(μ-OH)$_2$], M = Rh or Ir, to give [M(tmtaaH)(COD)], which give the dicarbonyl derivatives, [M(tmtaaH)$(CO)_2$], on exposure to CO. The COD and dicarbonyl derivatives, M = Rh, are methylated with MeOTf at the β-carbon site of the imidinate ring, giving [Rh(tmtaaHMe)$(L_2)]^+$, where L_2 = COD or $(CO)_2$. The crystal structure of [Rh(tmtaaHMe)$(CO)_2$][OTf] shows that the site of methylation is the imidinate ring that contains the Rh$(CO)_2$ fragment. Protonation by HOTf also occurs at the β-carbon site of the imidinate ring, assumed to be the ring that contains the Rh(L_2) fragment. The dicarbonyls are deprotonated by LiN$(SiMe_3)_2$ in thf, giving [M$(CO)_2$(tmtaa)Li(thf)]. A crystal structure of M = Rh shows an intramolecular Li−Rh distance of 2.635(10) Å and an intermolecular Rh···Rh contact distance between two molecular units of 3.198(1) Å that align along their molecular *z*-axis. Addition of MeI to [M$(CO)_2$(tmtaa)Li(thf)] yields [M(tmtaaMe)$(CO)_2$], where the methyl group is attached to the imidinate ring that contains the Li(thf) fragment, as shown by X-ray crystallography. The [M(tmtaaH)$(CO)_2$] reacts with half an equivalent of [M_2(COD)$_2$(μ-OH)$_2$] to give the mixed dimetal complexes [M$(CO)_2$(tmtaa)M′(COD)], where M,M′ is either Rh,Rh or Rh,Ir, which react with CO to give [MM′(tmtaa)$(CO)_4$].

Introduction

The dianion of 7,16-dihydro-6,8,15,17-tetramethyldibenzo-[*b*,*i*][1,4,8,11]tetraazacyclotetradecine, the systematic name for 6,8,15,17-tetramethyldibenzotetraaza[14]annulene, abbreviated tmtaa, has been studied extensively as a ligand in d-transition metal chemistry since the free base, tmtaaH_2, was prepared in synthetically useful amounts.[1,2] Most of the d-transition metal derivatives contain only one metal in the planar pocket defined by the four nitrogen atoms,[3,4] but a small number of dimetal derivatives of the type [(tmtaa)M$_2$(L)$_n$] have been described.[5] The free base, tmtaaH_2, has a saddle shape in the solid state with C_{2v} symmetry, and the monometal complexes generally have been shown or are assumed to have a similar shape.[3,4,6] However, the saddle shape is not universally observed since complexes such as [Pd(tmtaa)][7] and [*trans*-Ru$(PR_3)_2$(tmtaa)], PR_3 = PPh_2Me[8] or PPh_3,[9] have been observed in which the ligand has an open steplike conformation. The platinum complex, [Pt(tmtaa)], crystallizes in two polymorphs, one of which has a saddle shape and the other an open steplike conformation; these authors also show that the palladium complex is also dimorphic.[10] Thus, the conformation of the ligand is rather flexible and is driven by the electronic requirements of the d-transition metal, the steric requirements of the other ligands, and crystal packing effects. The dianion is a 14-membered ring with 24 π-electrons (4*n*, where *n* = 6) and therefore not Hückel aromatic, and the negative charge is not delocalized over the entire dianion. The negative charge is carried by the four nitrogen atoms (−0.98) and by the two β-carbons, NC_α(Me)-C_β(H), in the imidinate ring (−0.24); the α-carbons carry a positive charge (+0.40).[11,12] Thus, the HOMO of the dianion

* To whom correspondence should be addressed. E-mail: raandersen@lbl.gov.

† University of California.

‡ Universidad de Castilla−La Mancha.

(1) Goedken, V. L.; Molin-Case, J.; Whang, Y. *Chem. Commun.* **1973**, 337.

(2) Goedken, V. L.; Weiss, M. C.; Place, D.; Dabrowiak, J. *Inorg. Synth.* **1980**, *20*, 115.

(3) (a) Cotton, F. A.; Czuchajowska, J. *Polyhedron* **1990**, *9*, 2553. (b) Mountford, P. *Chem. Soc. Rev.* **1998**, *27*, 105.

(4) (a) Housemaker, C. E.; Ramage, D. L.; Kretz, C. M.; Shortz, J. T.; Pilato, R. L.; Geoffroy, G. L.; Rheingold, A. L.; Haggerty, B. S. *Inorg. Chem.* **1992**, *31*, 4453. (b) Solari, E.; De Angelis, S.; Floriani, C.; Chesi-Villa, A.; Rizzoli, C. *Inorg. Chem.* **1992**, *31*, 96. (c) Ciurli, S.; Floriani, C.; Chesi-Villa, A.; Guastini, C. *Inorg. Chem.* **1992**, *31*, 2520. (d) Hao, S.; Edema, J. J. H.; Gambarotta, S.; Bensimon, C. *Inorg. Chem.* **1992**, *31*, 2676. (e) Floriani, C.; Ciurli, S.; Chesi-Villa, A.; Guastini, C. *Angew. Chem., Int. Ed. Engl.* **1987**, *26*, 70. (f) Black, D. G.; Swenson, D. C.; Jordan, R. F.; Rogers, R. D. *Organmetallics* **1995**, *14*, 3539. (g) Klose, A. Solari, E.; Floriani, C.; Chesi-Villa, A.; Rizzoli, C. *Chem. Commun.* **1997**, 2297. (h) Nikonov, G. I.; Blake, A. J.; Mounford, P. *Inorg. Chem.* **1997**, *36*, 1107. (i) Klose, A. Solari, E.; Floriani, C.; Geremia, S.; Randaccio, L. *Angew. Chem., Int. Ed. Engl.* **1998**, *37*, 148. (j) Hesschenbrouck, J.; Solari, E.; Scopelliti, R.; Floriani, C.; Re, N. *J. Organomet. Chem.* **2000**, *596*, 77.

(5) (a) Gordon, G. C.; DeHaven, P. W.; Weiss, M. C.; Goedken, V. L. *J. Am. Chem. Soc.* **1978**, *100*, 1003. (b) Kadish, K. M.; Bottomley, L. A.; Schaeper, D.; Tsutsui, M.; Bobsein, R. L. *Inorg. Chem. Acta* **1979**, *36*, 219. (c) Cotton, F. A.; Czuchajowska, J. *J. Am. Chem. Soc.* **1991**, *113*, 3427.

(6) Goedken, V. L.; Pluth, J. J.; Peng, S. M.; Bursten, B. *J. Am. Chem. Soc.* **1976**, *98*, 8014.

(7) Tsutsui, M.; Bobsein, R. L.; Cash, J.; Pettersen, R. *Inorg. Chem.* **1979**, *18*, 758.

(8) Cotton, F. A.; Czuchajowska, J. *Polyhedron* **1990**, *9*, 1221.

(9) Luo, L.; Stevens, E. D.; Nolan, S. P. *Inorg. Chem.* **1996**, *35*, 252.

(10) Paul, R. L.; Gheller, S. F.; Heath, G. A.; Hockless, D. C. R.; Rending, L. M.; Sterns, M. *J. Chem. Soc., Dalton Trans.* **1997**, 4143.

(11) Tatsumi, K.; Hoffmann, R. *Inorg. Chem.* **1981**, *20*, 3771.

10.1021/om060039y CCC: $33.50
Publication on Web 06/23/2006

Scheme 1

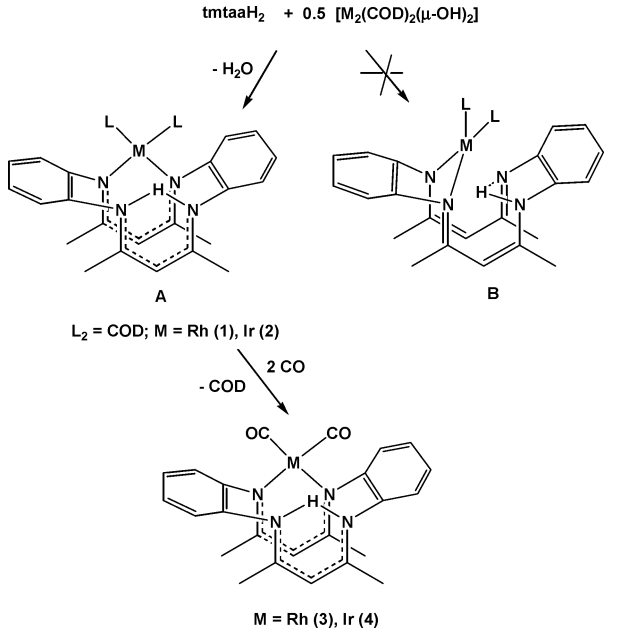

is a good σ-donor, but significant negative charge is located on the β-carbons. This molecular orbital model is useful in rationalizing the chemistry of the metal complexes of this ligand.

In this article, we describe a general synthesis of monometal complexes of Rh(I) and Ir(I), [M(tmtaaH)(L_2)], where (L_2) is COD or $(CO)_2$, their reactions with electrophiles, Me^+, H^+, and Li^+, and more importantly, a selective synthesis of the dimetal complexes [(ML,M′L′)(tmtaa)].

Results and Discussion

Synthesis of [M(tmtaaH)(L_2)]. The starting materials used in this work, [M(tmtaaH)(COD)], M = Rh (**1**) or Ir (**2**) in Scheme 1, are prepared in high yield by dissolving a 2:1 mixture of $tmtaaH_2$ and the hydroxide-bridged dimer [$Rh_2(COD)_2(\mu$-$OH)_2$] in toluene. The complexes may be crystallized from toluene as yellow, M = Rh, or orange, M = Ir, crystals in high yield. When the reaction is conducted in C_6D_6 in an NMR tube, and monitored by ^{1}H NMR spectroscopy, the reaction is quantitative over 4 h (Rh) or 14 h (Ir). In addition, a resonance for water is observed at δ = 0.5 ppm in each case. Two structural isomers are conceivable for these complexes as represented by **A** and **B** in Scheme 1. Assuming that the N−H proton is exchanging sites between the two adjacent nitrogen positions, both isomers have C_s symmetry, but they can be distinguished by ^{1}H and ^{13}C NMR spectroscopy. In **A**, the mirror plane of symmetry contains the imidinate β-CH group, making them chemically inequivalent, whereas in **B** the mirror plane of symmetry makes them chemically equivalent. The ^{1}H NMR spectra of **1** and **2** have two β-CH singlets at δ 4.89 and 4.62 (M = Rh) and δ 4.91 and 4.57 (M = Ir). The ^{13}C{^{1}H} NMR spectra also show two singlets at δ 99.9 and 99.5 (M = Rh) and δ 101.0 and 99.8 (M = Ir) for **1** and **2**. This pattern is consistent only with isomer **A**.

The COD ligand is displaced by brief exposure of **1** and **2** to carbon monoxide, yielding the dicarbonyl adducts **3** and **4**, respectively. These adducts form yellow crystals from toluene, M = Rh (**3**), or thf, M = Ir (**4**). Both complexes show two CO stretching frequencies, M = Rh, ν(CO) = 2061 and 1987 cm^{-1}, and M = Ir, ν(CO) = 2050 and 1966 cm^{-1}, in the solid state, consistent with the presence of a C_{2v} M(CO)$_2$ fragment (C_s for the molecule). The patterns of the resonances in the ^{1}H and ^{13}C{^{1}H} NMR spectra of **3** and **4** are similar to those found in **1** and **2**, suggesting that their stereochemistry is as shown in **A**, Scheme 1. The ORTEP diagram shown in Figure 1 proves this deduction for **3**. To see if the N−H functional group is interacting with the rhodium atom or if the NH···N site exchange is slow on the NMR time scale, the low-temperature ^{1}H NMR spectrum of **3** was examined to −80 °C in C_7D_8. No change in the chemical shift of the NH resonance at δ +12.4 is observed, nor is any Rh−H coupling observed at −80 °C.

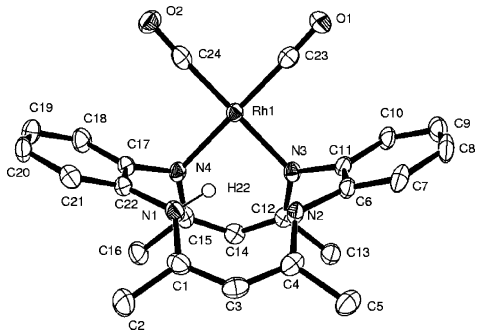

Figure 1. ORTEP diagram of [Rh(tmtaaH)$(CO)_2$], **3**. The ellipsoids are 50% probability surfaces except for the hydrogen atom, which is arbitrary. All non-hydrogen atoms are refined anisotropically, and the hydrogens are placed in calculated positions, except for the hydrogen atom H22 on N1, which is refined isotropically.

The molecular structure of **3** is shown in the ORTEP diagram in Figure 1. The crystal data are listed in Table 1, and some important bond lengths and bond angles are shown in Table 2; Table 3 lists the dihedral angles for this and related structures. The geometry is related to that of [Rh_2(tmtaa)$(CO)_4$],[5] in which a Rh$(CO)_2$ fragment is replaced by a hydrogen atom. The hydrogen atom is attached to N1 with a refined distance of 0.94(7) Å. The geometry around N2 is planar since the angles sum to 360° and the hydrogen atom on N1 is in the plane defined by N1−C1−C3−C4−N2, pointing toward Rh, with Rh1···H22 = 2.82(7) Å, and N2, with N2···H22 = 2.03(6) Å. The Rh−N distances, 2.043(2) and 2.046(3) Å, are slightly shorter than the average distance in [Rh_2(tmtaa)$(CO)_4$] of 2.071(4) Å. The Rh−C(CO) distances in these two structures are equal, 1.864(3) Å. The geometry around Rh is nearly square planar, as shown by the angles listed in Table 2.

An interesting feature of the molecular structure is the distortion of the tmtaa ligand in the neutral, monometal, and dimetal structures, as shown by the dihedral angles listed in Table 3. The distortions are described as α- or β-angles, as defined in the footnote to Table 3. The neutral free base and the imidinate fragment that retains the proton have similar β-angles. However, this angle increases to 76° in the imidinate fragment that contains the Rh$(CO)_2$ fragment. This is presumably due to the overlap requirement of the $d_{x^2-y^2}$ orbital as it forms a bond with the σ-orbitals on N3 and N4. The dihedral angle formed by the intersection of the planes defined by N3−Rh1−N4 and the N3−C12−C14−C15−N4 planes is 21° in the direction of N2−N1−H22. In [Rh_2(tmtaa)$(CO)_4$], the β-angle is not calculated, but it is said that "the N atom lone pairs are almost normal to the N4 plane".[5] The shortest intermolecular Rh···Rh contact distance is 5.58 Å, longer than that in [Rh_2-(tmtaa)$(CO)_4$] of 4.98 Å. The angles referred to as α change by an insignificant amount (2−4°) on going from the neutral ligand to **3**, and the "saddle angle" in both solid state structures is essentially the same.

(12) Giannici, L.; Solari, E. DeAngelio, S.; Ward, T. R.; Floriani, C.; Chiesi-Villa, A.; Rizzoli, C. *J. Am. Chem. Soc.* **1995**, *117*, 5801.

Table 1. Crystal Data for 3, 6, 9, and 11

	3	**6**	**9**	**11**
formula	$C_{24}H_{23}N_4O_2Rh$	$C_{26}H_{26}N_4O_5SF_3Rh$	$C_{28}H_{30}LiN_4O_3Rh$	$C_{25}H_{25}N_4O_2Rh$
fw	502.37	666.48	580.41	516.40
space group	$P2_1/n$	$P2_12_12_1$	$P2_1/n$	$P2_1/n$
a (Å)	11.894(1)	9.8907(9)	11.504(2)	9.702(1)
b (Å)	10.114(1)	10.1410(9)	16.972(3)	13.431(1)
c (Å)	18.139(1)	27.449(2)	14.306(3)	18.114(2)
β (deg)	93.180(2)		109.382(3)	100.745(1)
V (Å^3)	2178.6(4)	2753.2(4)	2643.9(9)	2319.0(4)
Z	4	4	4	4
ρ_{calc} (g/cm^3)	1.532	1.608	1.463	1.479
μ(Mo Kα)$_{calc}$ (cm^{-1})	8.1	7.6	6.8	7.6
size (mm)	0.20 × 0.18 × 0.06	0.06 × 0.04 × 0.04	0.18 × 0.18 × 0.15	0.11 × 0.08 × 0.07
temp (K)	125(2)	155(1)	140(2)	113(1)
scan type, θ_{max}	ω, 24.70	ω, 22.0	ω, 24.76	ω, 25.4
no. of reflns integrated	9390	10 995	11 499	10 928
no. of unique reflns, R_{int}	3596, 0.043	2612, 0.041	4323, 0.082	2971, 0.032
no. of good reflns	2865 ($I > 2.00\ \sigma(I)$)	2700 ($I > 3.00\ \sigma(I)$)	2846 ($I > 2.00\ \sigma(I)$)	3002 ($I > 3.00\ \sigma(I)$)
no. of variables	288	361	338	289
transmn range	0.90	0.82	0.98	0.86
R_1	0.037	0.030	0.054	0.049
wR_2	0.093	0.034	0.117	0.066
R_{all}	0.053	0.046	0.099	0.075
GOF	1.021	1.14	0.985	1.18

Table 2. Some Important Bond Distances (Å) and Angles (deg) for 3, 6, 9, and 11

compound **3**		compound **6**		compound **9**		compound **11**	
			Bond Distances				
Rh1−N3	2.046(3)	Rh1−N3	2.085(4)	Rh1−N1	2.034(5)	Rh1−N3	2.050(4)
Rh1−N4	2.043(3)	Rh1−N4	2.074(4)	Rh1−N2	2.058(5)	Rh1−N4	2.064(4)
Rh1−C23	1.870(4)	Rh1−C23	1.877(7)	Rh1−C23	1.861(6)	Rh1−C23	1.859(6)
Rh1−C24	1.858(4)	Rh1−C24	1.868(7)	Rh1−C24	1.852(7)	Rh1−C24	1.870(6)
N1−C1	1.338(5)	N1−C1	1.348(7)	N3−C12	1.332(7)	N1−C1	1.270(7)
N2−C4	1.323(5)	N2−C4	1.327(7)	N4−C15	1.319(7)	N2−C4	1.269(7)
N3−C12	1.329(5)	N3−C12	1.278(7)	N1−C2	1.336(7)	N3−C12	1.321(6)
N4−C15	1.322(5)	N4−C15	1.285(7)	N2−C4	1.324(7)	N4−C15	1.332(7)
N1−C22	1.413(5)	N1−C22	1.412(7)	N3−C11	1.405(7)	N1−C22	1.423(8)
N2−C6	1.412(5)	N2−C6	1.400(8)	N4−C17	1.408(7)	N2−C6	1.410(7)
N3−C11	1.433(5)	N3−C11	1.447(7)	N1−C22	1.446(7)	N3−C11	1.435(7)
N4−C17	1.443(5)	N4−C17	1.445(7)	N2−C6	1.445(7)	N4−C17	1.428(7)
		C14−C25	1.54(1)			C3−C25	1.525(8)
				Li1−N3	1.92(1)		
				Li1−N4	1.91(1)		
				Li1−Rh1	2.63(1)		
			Bond Angles				
N3−Rh1−N4	87.0(1)	N3−Rh1−N4	85.5(2)	N1−Rh1−N2	88.1(2)	N3−Rh1−N4	88.0(2)
C23−Rh1−C24	87.2(2)	C23−Rh1−C24	88.0(3)	C23−Rh1−C24	88.6 (3)	C23−Rh1−C24	85.9(3)
N3−Rh1−C23	92.9(2)	N3−Rh1−C23	92.9(2)	N1−Rh1−C23	91.4(2)	N3−Rh1−C23	93.2(2)
N4−Rh1−C24	92.8(2)	N4−Rh1−C24	93.7(2)	N2−Rh1−C24	91.6(2)	N4−Rh1−C24	92.7(2)
C11−N3−C12	117.9(3)	C11−N3−C12	122.7(5)	C2−N1−C22	115.7(5)	C11−N3−C12	117.1(5)
C15−N4−C17	117.6(3)	C15−N4−C17	122.3(5)	C4−N2−C6	116.8(5)	C15−N4−C17	115.4(3)
C1−N1−C22	126.3(3)	C1−N1−C22	127.7(5)	C11−N3−C12	122.4(5)	C1−N1−C22	120.6(5)
C4−N2−C6	125.1(3)	C4−N2−C6	124.9(5)	C15−N4−C17	122.8(5)	C4−N2−C6	120.5(5)
		C12−C14−C15	113.4(5)	N3−Li1−N4	97.7(5)	C1−C3−C4	110.8(5)
		C15−C14−C25	111.4(5)	N3−Li1−O3	128.4(6)	C1−C3−C25	11.0(5)
		C12−C14−C25	109.7(5)	N4−Li1−O3	113.8(5)	C4−C3−C25	114.7(5)

Reactions of [Rh(tmtaaH)(L$_2$)] with Electrophiles. Me$^+$ or H$^+$. The COD (**1**) and CO (**3**) complexes react with MeOTf ($MeOSO_2CF_3$) or HOTf ($HOSO_2CF_3$) to give the cationic species shown in Scheme 2. Addition of 1 molar equiv of MeOTf to **1** in CH_2Cl_2 gives a yellow solid whose empirical composition is [Rh(tmtaaHMe)(COD)][OTf], **5**. A cation of similar composition, [Rh(tmtaaHMe)(CO)$_2$][OTf], **6**, is obtained by addition of MeOTf to **3** followed by crystallization from a thf−pentane mixture.

There are three sites for electrophilic attack, the nitrogen lone-pair yielding **C** (Scheme 2) or the β-carbon atoms of the imidinate rings illustrated as **D** or **E** (Scheme 2), all of which carry a negative charge.[11,12] Structural isomer **C** has C_1 symmetry, whereas **D** and **E** have C_s symmetry assuming the NH···N tautomerization is rapid. In addition, the geometric isomers **D** and **E** have two possible orientations for the methyl group either exo or endo relative to the other imidinate ring. The ^{1}H NMR spectrum of **6** shows a new methyl resonance at δ 2.26 that appears as a doublet (J = 7 Hz), and the imidinate methine resonances appear as a quartet centered at δ 4.55 (J = 7 Hz) and a singlet at δ 4.92. This coupling pattern is diagnostic for isomer **D** or **E**, in which the methyl group is located on the β-carbon atom of the imidinate rings. Complex **5** has a similar pattern in the ^{1}H NMR spectrum, and the ^{13}C{^{1}H} NMR spectra for **5** and **6** are also similar. Furthermore, the imidinate C−Me groups in **5** and **6** appear as two equal area resonances in the ^{1}H NMR spectra. The exo stereochemistry is suggested by the lack of NOE between the two resonances at 2.26 (d) and 4.92 (s) in the ^{1}H−^{1}H NOESY experiment on **6**. Thus the site of electrophilic addition is not at the site of highest electron density

Table 3. Dihedral Angles in Selected tmtaa Structures[a]

	3	6	9	$tmtaaH_2$	$[Mo_2(tmtaa)(OAc)_2]$
α (deg)	18	18	13	20	9
	17	17	13	21	9
$-\beta$ (deg)	38	31	51	37	49
	76	64	57	37	49
ref	this work	this work	this work	5	13

[a] α and β angles are defined in the scheme below.

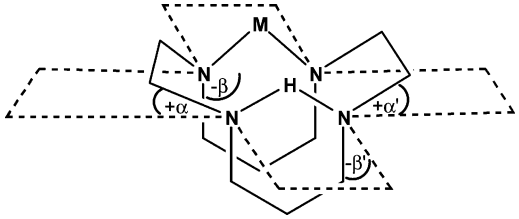

(the N site) but at the β-C(H) site, which is presumably the thermodynamic site preference. Although the site of electrophilic addition is the β-C(H) site, there are two different sites, one in which the imidinate ring contains the NH group and the other that contains the $Rh(L_2)$ fragment. It is not possible to distinguish between these two alternatives by NMR spectroscopy; the correct stereochemistry of **6** is illustrated by **D** (Scheme 2), as shown by X-ray crystallography. An ORTEP diagram of **6** is shown in Figure 2, and important bond angles and distances are listed in Table 2.

Comparison between the bond distances in **6** and **3** shows that the average Rh−N distance in **6** is 0.035 Å longer and the average N3−C12, N4−C15 distance is 0.044 Å shorter than the equivalent distances in **3**, while the average Rh−C(CO) distances are identical. The bond distance changes in the Rh1−N3−C12−C14−C15−N4 fragments in **6** and **3** are consistent with an increase in the local positive charge on the $Rh(CO)_2$ fragment in **6**, which results in a longer Rh−N distance and a shortening of the C−N distance as the C−N bond order increases. The bond angles in **6** and **3** are essentially identical in the two structures, as are the α-angles shown in Table 3. The β-angles, however, are different, since β_H and β_{Rh} are 7° and 12° smaller in **6**. Although the geometry around Rh is square-planar, the bond angles sum to 360°, the intersection of

Scheme 2

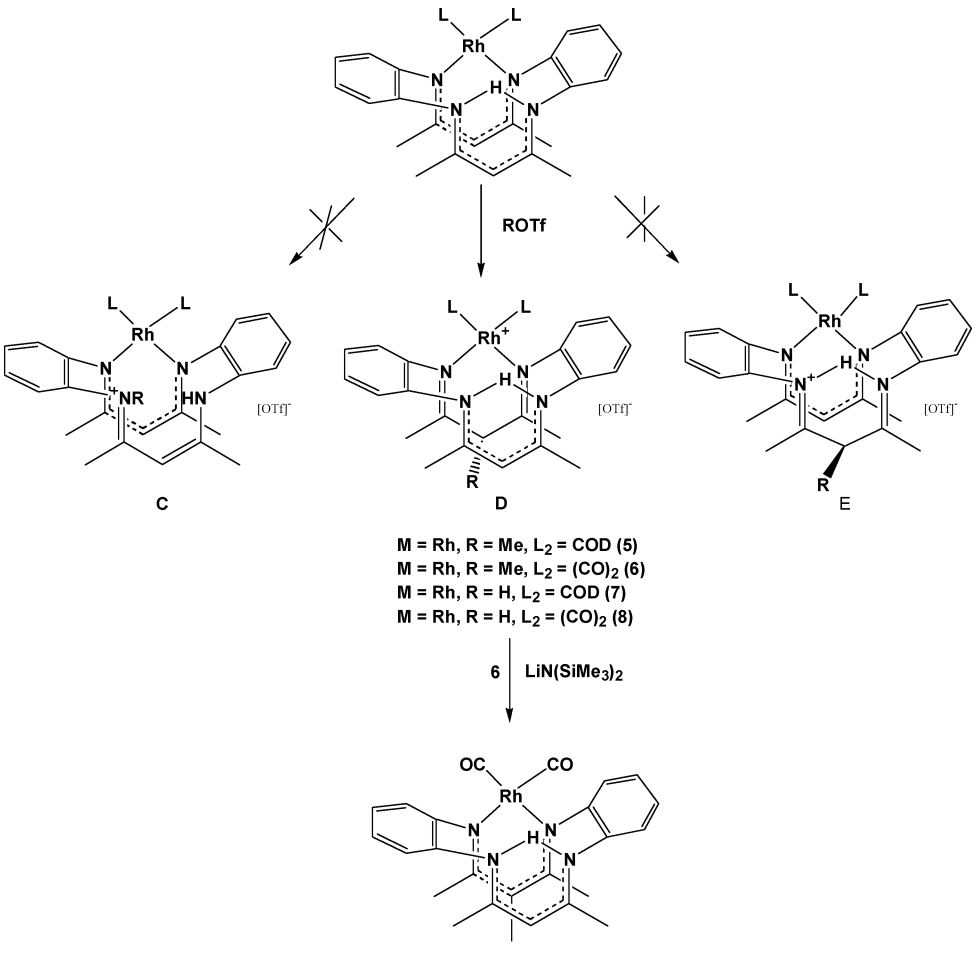

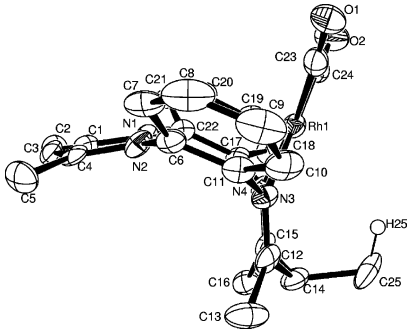

Figure 2. ORTEP diagram of [Rh(tmtaaHMe)(CO)$_2$][OTf], **6**. The ellipsoids are 50% probability surfaces except for the hydrogen atom, which is arbitrary. All non-hydrogen atoms are refined anisotropically, and all hydrogen atoms are placed in calculated positions and not refined. The triflate anion is not shown, but a complete ORTEP diagram is available as Supporting Information.

the planes defined by Rh1−N3−N4 and N3−C12−C15−N4 is 152°, and that between N3−C12−C15−N4 and C12−C13−C14 is 137°. The methyl group, C25, is exocyclic (Figure 2) with a short C−H···Rh contact distance of 2.77 Å; the hydrogen atom positions are not refined, but they are placed in idealized positions. The H···Rh contact distance is identical to that recently reported by Tilley and co-workers, where the hydrogen atom positions also were not refined.[14] The J_{Rh-H} and J_{Rh-C} couplings are not observed in either complex in solution and the H···Rh contact distance in the solid state structure of **6** is presumably a consequence of the six-membered ring in a boat configuration that orientates the C−H bond toward the filled d_{z^2} orbital on Rh.

Addition of 1 molar equiv of HOTf to [Rh(tmtaaH)(COD)], **1**, in thf, yields yellow plates of [Rh(tmtaaH$_2$)(COD)][OTf], **7**, on crystallization from thf. The dicarbonyl, **3**, behaves similarly, giving cation **8** as yellow crystals from thf. Again, three isomeric structures are possible, and these are illustrated in **C**, **D**, and **E**, where R = H. Isomers **D** and **E** are readily distinguished from **C** in the ^{1}H NMR spectrum since the CH$_2$ group in the β-site of an imidinate ring appears as an AB pattern in **8** at δ 4.64 with J = 16 Hz and 4.43 with J = 16 Hz, and the resonance of the β-CH group on the other imidinate ring appears as a singlet at δ 4.89. The NMR spectra of **7** are similar to those observed for **8**, and therefore isomer **D** is proposed (Scheme 2) by inference from the structure of **6** (Figure 2). The preference of H$^+$ for the β-C(H) site in metal complexes of the tmtaa has been observed by Goedken[6] and rationalized by Hoffmann.[11]

The protonation experiments do not, however, show whether the proton attacks a specific site or attacks all sites of negative electron density. A distinction is possible by using DOTf. Thus, addition of DOTf to a CD_2Cl_2 solution of **8** shows that deuterium is found in both nitrogen sites and in the β-CH sites. This is shown by carefully integrating the ^{1}H NMR spectrum of **3** in CD_2Cl_2, adding 1 equiv of DOTf at room temperature, then integrating the spectrum until the integrals due to the NH and CH resonances are constant relative to the intensity of the C−Me resonances. The result of this experiment shows that the intensity of the resonance due to the N−H (δ 12.6) decreases by 50%, the resonance due to the β-CH$_2$ (δ 4.5) decreases by 20% (10% in each site), and that due to the other β-CH site decreases by 20%. Given the accuracy of the integration, it is clear that D$^+$ is distributed over all sites of negative electron density and that the net preference for the N site is about the same as that for the C sites. This result may be interpreted by postulating that a rapid tautomeric equilibrium exchanges the N−H protons, which scrambles H and D between the two nitrogen atoms, while D$^+$ also attacks the β-C(H) site, generating C(H)(D). Thus, at 20 °C the protonation is not stereospecific.

Scheme 3

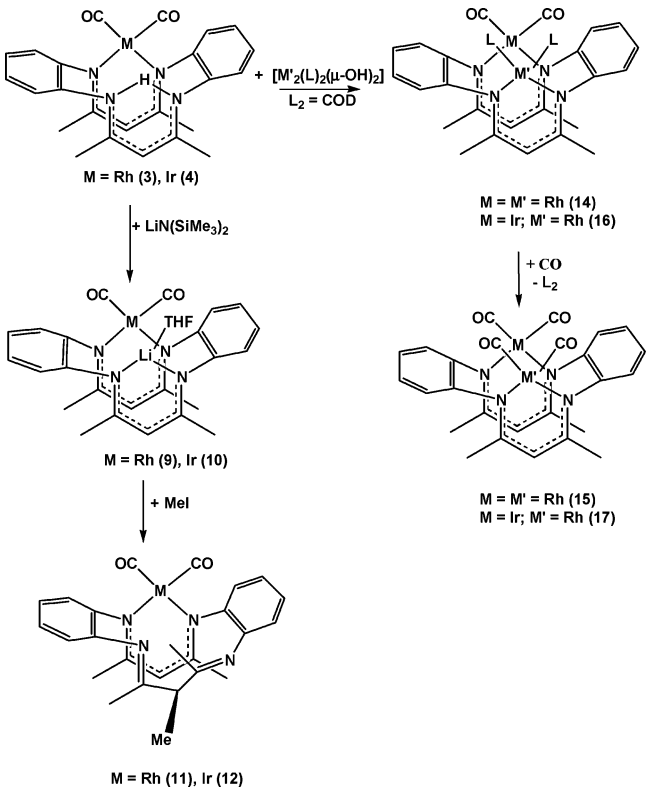

Reactions of [M(tmtaaH)(CO)$_2$] with the Proton Acceptor LiN(SiMe$_3$)$_2$. The N−H functional groups in **3** or **4** are acidic since they can be deprotonated by LiN(SiMe$_3$)$_2$ in thf at room temperature to give **9** and **10** (Scheme 3). Both complexes crystallize as red crystals from thf, and both complexes contain one thf per lithium. Unlike the other complexes described in this paper, which are stable to air and moisture, **9** and **10** are very air and moisture sensitive and the rhodium complex darkens on standing at room temperature, which is perhaps the reason **9** is the only complex for which an adequate elemental analysis is not obtained. The ^{1}H and ^{13}C{^{1}H} NMR spectra in C_6D_6 of **9** and **10** are similar and consistent with a contact ion-pair structure of C_s symmetry in which a Li(thf) fragment replaces a hydrogen atom in **3** and **4**. This deduction is shown to be correct by the X-ray structure of **9**.

An ORTEP diagram of the molecule [Rh(CO)$_2$(tmtaa)Li(thf)], **9**, is shown in Figure 3a. Crystal data are shown in Table 1, and bond distances and angles in Table 2. The intramolecular Rh−N, C−N, and C−C bond lengths are very similar to those found in complex **3**, Table 2. The geometry around rhodium is essentially square-planar, since the bond angles sum to 360°, but the geometry around the lithium is not trigonal-planar, since the angles sum to only 340°. Thus the lithium atom moves out of the trigonal plane defined by N3−N4−O3, forming a tetrahedral and four-coordinate lithium, since the Li···Rh distance is 2.635 Å. It seems reasonable to propose that this interaction is between the pair of electrons in the Rh d_{z^2} orbital and an empty sp_z-hybridized orbital on lithium. Thus, the interaction may be viewed as a donor−acceptor bond in which

(13) Kebaol, J. M.; Furet, E.; Guerchias, J. E.; LeMest, Y.; Saillard, J. Y.; Sala-Pala, J.; Toupet, L. *Inorg. Chem.* **1993**, *32*, 713.

(14) Krumper, J. R.; Gerisch, M.; Magistrato, A.; Rothlisberger, U.; Bergman, R. G.; Tilley, T. D. *J. Am. Chem. Soc.* **2004**, *126*, 12492.

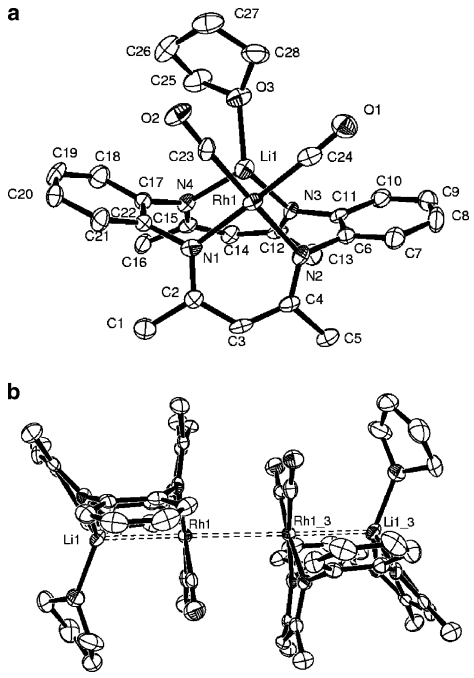

Figure 3. (a) ORTEP diagram of [Rh(CO)$_2$(tmtaa)Li(thf)], **9**. The ellipsoids are 50% probability surfaces. All non-hydrogen atoms are refined anisotropically, and all hydrogen atoms are placed in calculated positions. (b) ORTEP diagram showing two molecules of **9** in the unit cell. The complete packing diagram is available as Supporting Information.

negative charge density is transferred from rhodium to the electropositive lithium atom. This bond model is consistent with the increase in the CO stretching frequencies on going from [Rh(tmtaaH)(CO)$_2$], **3**, ν(CO) = 2061 and 1987 cm^{-1} to 2071 and 2013 cm^{-1} in [Rh(CO)$_2$(tmtaa)Li(thf)], **9**. Thus the Li(thf) fragment competes for electron density with carbon monoxide on the rhodium fragment. The geometry of the iridium complex, **10**, is assumed to be similar.

The Li−N distances of 1.914(11) and 1.922(11) Å, where the coordination number is three, are shorter than those found in [Li$_4$(tmtaa)$_2$(dme)$_3$], which range from 2.028(6) to 2.813(6) Å, where the coordination number ranges from four to six.[4d] The Li−O distance of 1.940(11) Å is in the range found for three-coordinate lithium.[15] Although the C−C and C−N distances do not change much on going from **3** to **9**, the tmtaa ligand undergoes a substantial reorganization. This is quantified by comparing the dihedral angles shown in Table 3 for **3** and **9**. Both α-angles open by 4−5°, making the saddle more open. The largest change is in the β-angles, which decreases by 5° for the fragment that contains the Rh(CO)$_2$ fragment but opens by 13° when H is replaced by Li(thf). These changes are presumably dictated by the need to maximize the overlaps between the nitrogen donor orbitals and the square-planar Rh(I) and tetrahedral Li(thf) fragments.

The big difference between the two structures of **3** and **9**, however, is not apparent by comparing the molecular structures in Figures 1 and 3a, but the difference appears when the crystal structures are examined, Figure 3b. In [Rh(tmtaaH)(CO)$_2$], **3**, the intermolecular Rh···Rh contact distance is 5.58 Å; a packing diagram is available in the Supporting Information. In contrast, the Rh(1)···Rh(1_3) contact distance between the two rhodium atoms of the individual [Rh(CO)$_2$(tmtaa)Li(thf)] molecules in the unit cell is 3.198 Å, 2.2 Å less than in **3**. In the monoclinic unit cell, the individual [Rh(CO)$_2$(tmtaa)Li(thf)] molecules are packed in an up−down fashion with the orientation Li−Rh···Rh−Li along the molecular *z*-axis as shown in Figure 3b; a packing diagram is available as Supporting Information. A similar packing is observed in [Rh$_2$(tmtaaH)(CO)$_4$]$^+$···[Rh$_2$(tmtaaH)(CO)$_4$]$^+$, where the Rh···Rh contact distance is 3.268 Å, only 0.21 Å shorter than the intramolecular Rh−Rh distance of 3.057 Å.[5] In this structure the orientation of the dimers is up−down, and the stacking of the dimetal fragments are [Rh(+)−Rh]···[Rh−Rh(+)] along the molecular *z*-axis.

The Rh···Rh contact distance in these two rather different molecular complexes differs by only 0.070 Å, with the shorter distance found in the Li−Rh complex. The Rh···Rh contact distance cannot be rationalized by a dipole−dipole interaction in the solid state since the orientation of the dipoles is repulsive. A qualitative molecular orbital description along the lines advanced by Gray and co-workers to account for weak Rh−Rh bonds in [Rh(CNR)$_4$]$_2^{2+}$ is applicable to the complexes described here.[16] In the isocyanide dimers the two Rh(I) square-planar fragments approach each other along their molecular *z*-axis with a Rh−Rh distance of 3.193 Å in [Rh$_2$(CNPh)$_8$]$^{2+}$. The Rh−Rh interaction is suggested to result from a combination of the d_{z^2} orbitals forming a bonding and an antibonding molecular orbital with a pair of electrons in each. Mixing the empty p_z orbital into the $(d_{z^2})^*$ orbital removes some of the antibonding character, resulting in a net Rh−Rh bonding interaction. A qualitatively similar bond model may be applied to **9**, in which the Li(thf)$^+$ uses its empty p_z orbital to remove electron density from the HOMO, the $(d_{z^2})^*$ orbital. The net result is that the Rh−Rh distance in these two very different molecules is identical since the frontier molecular orbitals are isolobal and presumably isoenergetic.

Reactions of [M(CO)$_2$(tmtaa)Li(thf))] with Me$^+$. Addition of MeI to either **9** or **10** in thf gives the neutral complexes that may be obtained from pentane as red crystals, M = Rh, **11**, or a yellow solid, M = Ir, **12**. The site of the methyl group can be either the N site or the β-C(H) site. These two possibilities are readily distinguishable since the β-C(Me)(H) group will give rise to a doublet, quartet pattern in the ^{1}H NMR spectrum. This pattern is observed for **11** and **12**, but, as above, the NMR spectra do not show which imidinate ring carries the β-C(H)(Me) group. The crystal structure of **11** is shown by the ORTEP diagram in Figure 4, which shows that the site of the methyl group, C25, is the β-carbon atom of the imidinate ring that contains the Li(thf) fragment in **9**. However, the stereochemistry of the N1−C1−C3−C4−N2 imidinate ring changes so that N1 and N2 have an anti orientation rather than a syn one, presumably to avoid the lone-pair repulsion in a syn orientation. In comparison with **3** the Rh1−N3−N4−C23−C24 fragment in each complex is essentially identical, but the average N1−C1 and N2−C4 distance in **11** is 0.060 Å shorter, since these bonds are now C=N bonds. In the crystal structure two individual [Rh(tmtaaMe)(CO)$_2$] molecules are orientated in an up−down fashion along the molecular *z*-axis, similar to **9**, Figure 3b, so that the Rh···Rh distance is 3.370(1) Å, 0.172 Å longer than in **9**.

The solid state structure of **11**, and presumably **12**, clearly shows that the molecule is without symmetry. In C_7D_8 solution, however, the ^{1}H NMR spectrum at 20 °C is consistent with a molecule of C_s symmetry since the α-C(Me) groups on the

(15) Setzer, W. N.; Schleyer. P. R. *Adv. Organomet. Chem.* **1985**, *24*, 353−451.

(16) (a) Lewis, N. S.; Mann, K. R.; Gordon, J. G., II; Gray, H. B. *J. Am. Chem. Soc.* **1976**, *98*, 7461. (b) Smith, D. C.; Miskowski, V. M.; Mason, W. R.; Gray, H. B. *J. Am. Chem. Soc.* **1990**, *112*, 3759.

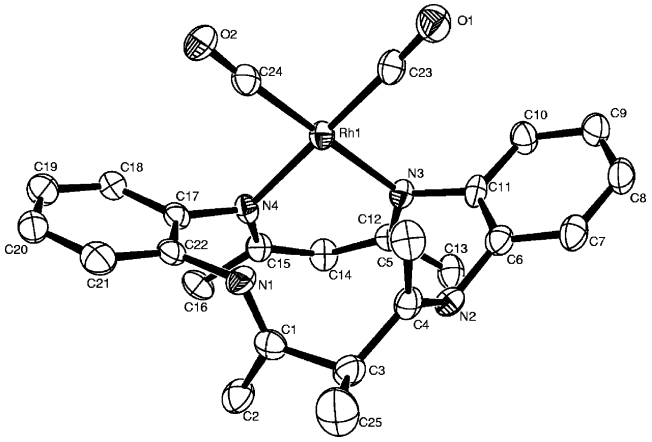

Figure 4. ORTEP diagram of [Rh(tmtaaMe)(CO)$_2$], **11**. The ellipsoids are 50% probability surfaces. All non-hydrogen atoms are refined anisotropically, and all hydrogens are placed in calculated positions, not refined, and not shown.

imidinate rings are pairwise chemically equivalent since they appear as single resonances (6 H each) at 1.80 and 1.77 ppm and the β-C(Me) resonance appears as a doublet at 1.20 ppm. As the temperature of the solution is lowered, the two single, sharp resonances broaden into three very broad resonances in an approximate 3:6:3 ratio by −50 °C, which yield four slightly broadened equal-area singlets at 2.22, 1.81, 1.61, and 1.18 ppm by −80 °C. Over this temperature range, the line shape of the doublet resonance due to the β-C(Me) does not change appreciably. Thus, at −80 °C the α-C(Me) resonances are chemically inequivalent, as observed in the solid state, Figure 4. The fluxional motion is presumably due to rotation about C3−C4 that introduces a time-averaged mirror plane of symmetry, resulting in chemical equivalence of C2, C5 and C13, C16 (Figure 4).

Deprotonation of cation **6** with LiN(SiMe$_3$)$_2$ yields the neutral complex [Rh(tmtaaMe)(CO)$_2$], **13**, which has the same empirical composition as **11**, R = Me, but is a different structural isomer (Scheme 2). The ^{1}H NMR spectrum shows that the N−H group is present, as is the β-CMe group, which is a singlet. Isomers **11** and **13** differ only in the substituents on the N and C sites and presumably the conformation of the imidinate rings since the proton in **13** forces the syn conformation, but it is unknown which proton is abstracted from cation **6**. Since the specific sites cannot be deuterated, this question cannot be answered by an experiment, but the results described earlier are consistent with deprotonation of the C−H rather than the N−H bond.

Reactions of [M(tmtaaH)(CO)$_2$] with the Proton Acceptor [Rh$_2$(COD)$_2$(μ-OH)$_2$]. Perhaps the most interesting set of reactions described in this paper are the proton abstractions from **3** and **4** by [Rh$_2$(COD)$_2$(μ-OH)$_2$], which eliminate water and form the dimetal complexes shown in Scheme 3. These reactions result in the specific synthesis of dimetal complexes in which the two metals and their ligands give a single isomer depending upon the identity of the starting reagents. Mixing [Rh(tmtaaH)(CO)$_2$], **3**, and [Rh$_2$(COD)$_2$(μ-OH)$_2$] in an NMR tube in C$_6$D$_6$ shows only resonances in the ^{1}H NMR spectrum of the individual reactants. Heating at 85 °C results in their disappearance and appearance of a new set of resonances, including one due to water (δ 0.5), over a 4−5 h period. Repeating the reaction on a synthetic scale yields [Rh(CO)$_2$(tmtaa)Rh(COD)], **14**, Scheme 3. The ^{1}H NMR spectrum is consistent with this structure since the NH resonance is absent and the COD resonances appear as six equal area resonances. Exposure of **14** to CO yields the known complex [Rh$_2$(tmtaa)(CO)$_4$], **15**, whose ^{1}H NMR spectrum is identical to that reported.[6] A similar reaction is observed on mixing [Ir(tmtaaH)(CO)$_2$], **4**, and [Rh$_2$(COD)$_2$(μ-OH)$_2$] in toluene and heating for 3 h. Cooling the mother liquor yields dark red crystals of [Ir(CO)$_2$(tmtaa)Rh(COD)], **16**. In this complex the CO ligands are attached to the iridium atom since they appear as a single resonance at δ 178 in the ^{13}C NMR spectrum, while in **14** the carbonyl resonance appears as a doublet at δ 188 with J_{Rh-C} = 67 Hz. This shows that the ligands on the d^8-metal fragments do not exchange positions during the synthesis. Exposure of **16** to an atmosphere of CO yields the tetracarbonyl derivative [Ir(CO)$_2$(tmtaa)Rh(CO)$_2$], **17**. When **16** is dissolved in C$_7$D$_8$ in an NMR tube and exposed to an atmosphere of CO, then heated to 70 °C, the only resonances observed in the spectrum are those due to free COD and **17**. When the ^{1}H NMR spectrum of isolated **17** in C$_6$D$_6$ is monitored over 15 h (20 °C) and 8 h (70 °C), no new resonances or intensity changes are observed. Thus **17** does not disproportionate to **15** and, by implication, [Ir$_2$(tmtaa)(CO)$_4$] under these conditions.

Table 4. ν CO Stretching Frequencies (Nujol mulls)

compound	ν CO stretching frequencies (cm^{-1})	average frequency (cm^{-1})
[Rh(tmtaaH)(CO)$_2$], **3**	2061, 1987	2024
[Ir(tmtaaH)(CO)$_2$], **4**	2050, 1966	2008
[Rh(tmtaaHMe)(CO)$_2$][OTf], **6**	2092, 2029	2060
[Rh(tmtaaH$_2$)(CO)$_2$][OTf], **8**	2097, 2024	2060
[Rh(CO)$_2$(tmtaa)Li(thf)], **9**	2071, 2013	2042
[Ir(CO)$_2$(tmtaa)Li(thf)], **10**	2039, 1981	2010
[Rh(tmtaaMe)(CO)$_2$], **11**	2052, 1985	2018
[Rh(tmtaaMe)(CO)$_2$], **13**	2055, 1992	2023
[Rh(CO)$_2$(tmtaa)Rh(COD)], **14**	2050, 1980	2015
[Ir(CO)$_2$(tmtaa)Rh(COD)], **16**	2032, 1957	1994
[Ir(CO)$_2$(tmtaa)Rh(CO)$_2$], **17**	2056, 2040, 2001, 1984	2020

Discussion of the CO Stretching Frequencies. The CO stretching frequencies of the complexes prepared in this paper are listed in Table 4. All of the complexes in Table 4 have C_s or lower symmetry, and the monometal complexes are expected to display two CO stretching frequencies, as observed. The average value of the two observed frequencies can be used to get information about the electron density at the M(CO)$_2$ fragment.

The average value of ν CO of **4**, M = Ir, is 16 cm^{-1} lower than that in the analogous rhodium complex, **3**. This is consistent with the well-known periodic trend that third-row transition metals are better π-bases than those in the second row. A similar trend is observed when the dimetal complexes **16** and **14** are compared; namely, the average value of ν CO in **16** is 21 cm^{-1} lower than that of **14**. When Li(thf)$^+$ replaces the NH protons forming **9** and **10**, the average ν CO increases by 18 cm^{-1} (M = Rh) and 2 cm^{-1} (M = Ir). This is consistent with Li(thf)$^+$ being a better acceptor than H$^+$, as mentioned earlier.

The protonated and methylated rhodium complexes **6** and **8** have an identical average ν CO stretching frequency that is 36 cm^{-1} higher than that in neutral **3**, consistent with the view that a cation is a poorer electron donor than a neutral molecule. The solid state structure of **6** shows that the Rh(CO)$_2$ fragment stabilizes the positive charge better than does a proton on the imidinate fragment, which is consistent with the increase in ν CO from **3** to **6**. The average ν CO for **13** of 2023 cm^{-1} is identical to that in **3**, showing that replacing a hydrogen atom by a methyl group in the imidinate fragment has a minor effect. However, the ν CO of **11**, an isomer of **13**, is 5 cm^{-1} lower than that in **13**, which shows that the ligands on the framework

of the macrocycle do have subtle effects on the global electron density in these complexes.

The CO stretching frequencies of the complexes described in this paper are an informative measure of the donor characteristics of the tmtaaH$^-$ ligand. Thus the average values of ν CO for the well-known acetylacetonate complexes are 2049 cm^{-1} in [Rh(acac)(CO)$_2$][17] and 2037 cm^{-1} in [Ir(acac)(CO)$_2$].[18] These values are 25−29 cm^{-1} higher than in **3** and **4**, respectively, clearly showing that tmtaaH$^-$ is a better donor than acac$^-$. Another comparison is the average ν CO value in the anion [Rh(oxalate)(CO)$_2$]$^-$, 2035 cm^{-1}, consistent with the tmtaaH$^-$ being a better donor than the oxalate dianion.[19]

On the other hand, tmtaaH$^-$ is a slightly poorer or comparable donor than that of a dithiocarbamate ligand, as shown by the average ν CO's in [Rh(RR′NCS$_2$)(CO)$_2$], R = R′ = Me (2038 cm^{-1}),[20] R = R′ = Et (2031 cm^{-1}),[20] R = Me, R′ = Ph (2020 cm^{-1}).[21] The tmtaaH$^-$ is a better donor than the bidentate sulfur−nitrogen ligand in the rhodium pyrimidine thiolate complex, where the average value of ν CO is 2038 cm^{-1}.[22] Similarly, tmtaaH$^-$ is a better donor than the bidentate oxygen−nitrogen ligands, 8-oxyquinoline or salicylaldimine [M(oxyquinoline)-(CO)$_2$], M = Rh, ν CO = 2040 cm^{-1}; M = Ir,[23] ν CO = 2032 cm^{-1}, and [M(salicylaldimine)(CO)$_2$], M = Rh, ν CO = 2044 cm^{-1}; M = Ir,[24] ν CO = 2028 cm^{-1}. One more comparison is revealing; the average ν CO in [RhCp(CO)$_2$][25] and [IrCp(CO)$_2$][26] are 2019 and 2007 cm^{-1}, respectively. These values are close to those in **3** (2024 cm^{-1}) and **4** (2008 cm^{-1}), showing that tmtaaH$^-$ and Cp$^-$ are comparable donors.

Conclusion

The synthetic method outlined in this paper is general for the preparation of monorhodium and -iridium complexes of the type [M(tmtaaH)(L$_2$)]. The synthetic route is applicable for the stereospecific synthesis of dimetal derivatives in which the macrocyclic dianion supports Rh,Rh or Rh,Ir fragments. The synthetic methodology yields complexes with a specific stereochemistry that will be used to study the nature of the intra- and intermolecular interactions between these d^8−d^8 complexes and how these interactions influence the reaction chemistry. These studies will be described in due course.

Experimental Section

General Procedures. All reactions and product manipulations were carried out under dry nitrogen using standard Schlenk and glovebox techniques. All organic solvents were distilled prior to use. [Rh$_2$(COD)$_2$(μ-OH)$_2$],[27] [Ir$_2$(COD)$_2$(μ-OH)$_2$],[28] and tmtaaH$_2$[2] were prepared according to the literature methods. All other chemicals were purchased from Aldrich and used as received. Infrared spectra were obtained as Nujol mulls. ^{1}H and ^{13}C NMR spectra were recorded on a Bruker AVB-400, AVQ-400, or 200 Mercury Varian Fourier transform spectrometer. Trace amounts of protonated solvents were used as references, and chemical shifts are reported in units of parts per million relative to SiMe$_4$.

[Rh(tmtaaH) (COD)] (1). To a mixture of [Rh$_2$(COD)$_2$(μ-OH)$_2$] (0.284 g, 0.62 mmol) and tmtaaH$_2$ (0.428 g, 1,24 mmol) was added toluene. The suspension was stirred at room temperature for 4 h and then filtered. The solvent was removed under vacuum and the yellow residue washed with Et$_2$O (yield 0.479 g, 69%). ^{1}H NMR (C$_6$D$_6$, rt): δ 12.42 (s, 1 H, NH), 6.84 (m, 8 H, Ar), 4.89 (s, 1 H), 4.62 (s, 1 H), 4.30 (m, 2 H, COD), 2.71 (m, 2 H, COD), 2.28 (m, 2 H, COD), 1.94 (m, 2 H, COD), 1.75 (s, 6 H, Me), 1.64 (8 H, Me, COD), 1.27 (m, 2 H, COD). ^{13}C{^{1}H} NMR: δ 158.6 (s, *C*-Me), 157.2 (s, *C*-Me), 145.3 (s, ipsoAr), 141.8 (s, ipsoAr), 124.8 (s, Ar), 124.2 (s, Ar), 123.4 (s, Ar), 121.9 (s, Ar), 99.9 (s, CH), 99.5 (s, CH), 80.7 (d, $^1J_{Rh-C}$ = 13.2 Hz, COD), 76.3 (d, $^1J_{Rh-C}$ = 12.6 Hz, COD), 30.8 (COD), 30.3 (s, COD), 23.8 (s, Me), 20.8 (s, Me). Anal. Calcd for C$_{30}$H$_{35}$N$_4$Rh: C, 64.97; H, 6.36; N, 10.10. Found: C, 65.03; H, 6.45; N, 10.02.

[Ir(tmtaaH)(COD)] (2). To a mixture of [Ir$_2$(COD)$_2$(μ-OH)$_2$] (0.151 g, 0.24 mmol) and tmtaaH$_2$ (0.164 g, 0,48 mmol) was added toluene. The suspension was stirred at room temperature for 14 h and then filtered. The solvent was partially evaporated under vacuum and the solution kept at −20 °C for 1 day to yield a crystalline orange compound (0.200 g, 64%). ^{1}H NMR (C$_6$D$_6$, rt): δ 12.05 (s, 1 H, NH), 6.89 (m, 8 H, Ar), 4.91 (s, 1 H), 4.57 (s, 1 H), 4.18 (m, 2 H, COD), 2.45 (m, 2 H, COD), 2.22 (m, 2 H, COD), 1.87 (m, 2 H, COD), 1.71 (s, 6 H, Me), 1.62 (8 H, Me, COD), 1.15 (m, 2 H, COD). ^{13}C{^{1}H} NMR: δ 159.0 (s, *C*-Me), 157.2 (s, *C*-Me), 144.9 (s, ipsoAr), 141.9 (s, ipsoAr), 124.8 (s, Ar), 124.7 (s, Ar), 123.4 (s, Ar), 121.6 (s, Ar), 101.0 (s, CH), 99.8 (s, CH), 63.1 (s, COD), 59.9 (s COD), 31.7 (COD), 30.9 (s, COD), 23.8 (s, Me), 20.7 (s, Me). Anal. Calcd for C$_{30}$H$_{35}$N$_4$Ir: C, 55.96; H, 5.47; N, 8.70. Found: C, 56.59; H, 5.52; N, 8.53.

[Rh(tmtaaH)(CO)$_2$] (3). Carbon monoxide was bubbled through a suspension of **1** (0.153 g, 0.27 mmol) in pentane at 0 °C for 5 min, the suspension was stirred under CO atmosphere for 1 h, and then the solid was separated by filtration. The residue was extracted with toluene and the solution kept at −20 °C for 2 days to yield pale yellow crystals (0.105 g, 75%). IR (ν C−O): 2061 (vs), 1987 (vs). ^{1}H NMR (C$_6$D$_6$, rt): δ 12.61 (s, 1 H, NH), 7.10 (m, 2 H, Ar), 6.90 (m, 4 H, Ar), 6.80 (m, 2 H, Ar), 4.92 (s, 1 H), 4.54 (s, 1 H), 1.70 (s, 6 H, Me), 1.59 (s, 6 H, Me). ^{13}C{^{1}H} NMR (toluene, rt): δ 186.2 (d, $^1J_{Rh-C}$ = 66.8 Hz, CO), 160.2 (s, *C*-Me), 157.3 (s, *C*-Me), 148.5 (s, ipsoAr), 141.3 (s, ipsoAr), 123. 4 (s, Ar), 123. 3 (s, Ar), 123.2 (s, Ar), 100.1 (s, CH), 99.2 (s, CH), 21.7 (s, Me). Anal. Calcd for C$_{24}$H$_{23}$N$_4$O$_2$Rh: C, 57.38; H, 4.62; N, 11.15. Found: C, 57.16; H, 4.69; N, 11.05.

[Ir(tmtaaH)(CO)$_2$] (4). A solution of complex **2** in THF (0.105 g, 0.16 mmol) was stirred under a CO atmosphere for 2 h. The solution was cooled to − 30 °C for 1 day to yield pale yellow crystals (0.064 g, 66%). IR (ν C−O): 2050 (vs), 1966 (vs). ^{1}H NMR (C$_6$D$_6$, rt): δ 12.39 (s, 1 H, NH), 7.04 (m, 2 H, Ar), 6.86 (m, 4 H, Ar), 6.74 (m, 2 H, Ar), 4.91 (s, 1 H), 4.48 (s, 1 H), 1.64 (s, 6 H, Me), 1.50 (s, 6 H, Me). ^{13}C{^{1}H} NMR: δ 176.3 (s, CO), 160.7 (s, *C*-Me), 157.8 (s, *C*-Me), 147.5 (s, ipsoAr), 141.6 (s, ipsoAr), 125.9 (s, Ar), 123. 4 (s, Ar), 123.3 (s, Ar), 123.1 (s, Ar), 102.3 (s, CH), 99.4 (s, CH), 21.9 (s, Me), 20.2 (s, Me). Anal. Calcd for C$_{24}$H$_{23}$N$_4$O$_2$Ir: C, 48.72; H, 3.91; N, 9.46. Found: C, 48.67; H, 3.90; N, 9.40.

[Rh(tmtaaHMe)(COD)][OTf] (5). To a solution of **1** (0.239 g, 0.43 mmol) in CH$_2$Cl$_2$ was added MeOTf (0.070 g, 0.43 mmol), and the solution was stirred at room temperature for 2 h. The solvent was removed under vacuum, and the residue was washed with THF to yield complex **5** as a yellow solid (0.285 g, 92%). ^{1}H NMR (CD$_2$Cl$_2$, rt): δ 12.34 (s, 1 H, NH), 7.20 (m, 4 H, Ar), 7.06 (m, 2 H, Ar), 6.61 (m, 2 H, Ar), 4.92 (s, 1 H, CH), 4.23 (q, $^3J_{H-H}$ =

(17) Bonati, F.; Wilkinson, G. *J. Chem. Soc.* **1964**, 3156.
(18) Bonati, F.; Ugo, R. *J. Organomet. Chem.* **1968**, *11*, 341.
(19) Real, J.; Bayón, J. C.; Lahoz, F. *J. Chem. Commun.* **1989**, 1889.
(20) Cotton, F. A.; McCleverty, J. A. *Inorg. Chem.* **1964**, *10*, 1398.
(21) Elduque, A.; Finestra, C.; López, J. A.; Lahoz, F. J.; Merchan, F.; Oro, L. A.; Pinillos, M. T. *Inorg. Chem.* **1998**, *37*, 824.
(22) Rojas, S.; Fierro, J. L. G.; Fandos, R.; Rodríguez, A.; Terreros, P. *J. Chem. Soc., Dalton Trans.* **2001**, 2316.
(23) Ugo, R.; LaMonica, G.; Cenini, S.; Bonati, F. *J. Organomet. Chem.* **1968**, *11*, 159.
(24) Cozens, R. J.; Murria, K. S.; West, B. O. *J. Organomet. Chem.* **1971**, *27*, 399.
(25) Fischer, E. O.; Bittler, K. *Z. Naturforsch.* **1961**, *16b*, 225.
(26) Fischer, E. O.; Brenner, K. S. *Z. Naturforsch.* **1962**, *17b*, 774.
(27) (a) Usón, R.; Oro, L. A.; Cabeza, J. A. *Inorg. Synth.* **1985**, *23*, 126. (b) Selent, D.; Ramm, M. *J. Organomet. Chem.* **1995**, *485*, 135.
(28) Green, L. M.; Meek, D. W. *Organometallics* **1989**, *8*, 659.

7.41 Hz, 1 H, CH), 4.13 (m, 2 H, COD), 2.83 (m, 2 H, COD), 2.65 (d, $^3J_{H-H}$ = 7.41 Hz, 3 H, Me), 2.38 (m, 2 H, COD), 2.08 (m, 8 H, Me + COD), 1.99 (6 H, Me), 1.86 (m, 2 H, COD), 1.64 (m, 2 H, COD). $^{13}C\{^1H\}$ NMR: δ 183.8 (s, ipsoAr), 160.9 (s, *C*-Me), 140.3 (s, *C*-Me), 137.3 (s, ipsoAr), 127.9 (s, Ar), 125.7 (s, Ar), 124.8 (s, Ar), 120.6 (s, Ar), 100.8 (s, CH), 89.0 (d, $^1J_{Rh-C}$ = 12.6 Hz, COD), 83.5 (d, $^1J_{Rh-C}$ = 11.8 Hz, COD), 54.4 (s, CMe), 31.0 (COD), 30.6 (s, COD), 24.9 (s, Me), 24.1 (s, Me), 21.4 (s, Me). $^{19}F\{^1H\}$ NMR: δ −79.3 (s, CF_3). Anal. Calcd for $C_{32}H_{38}F_3N_4O_3RhS$: C, 53.48; H, 5.33; N, 7.79. Found: C, 52.95; H, 5.34; N, 7.68.

[Rh(tmtaaHMe)(CO)$_2$][OTf] (6). To a solution of **3** (0.191 g, 0.38 mmol) in CH_2Cl_2 was added MeOTf (0.062 g, 0.38 mmol), and the solution was stirred at room temperature for 2 h. The solvent was removed under vacuum and the residue crystallized by slow diffusion of pentane into a THF solution (0.179 g, 71%). IR (ν C−O): 2092 (vs), 2029 (vs). ^1H NMR (CD_2Cl_2, rt): δ 12.62 (s, 1 H, NH), 7.32 (m, 6 H, Ar), 7.05 (m, 2 H, Ar), 4.92 (s, 1 H), 4.55 (q, 1 H, $^3J_{H-H}$ = 7.02 Hz, 1 H), 2.26 (d, 3 H, $^3J_{H-H}$ = 7.02 Hz, 1 H), 2.17 (s, 6 H, Me), 2.00 (6 H, Me). $^{13}C\{^1H\}$ NMR: δ 189.2 (s, ipsoAr), 182.5 (d, $^1J_{Rh-C}$ = 70.4 Hz, CO), 161.6 (s, *C*-Me), 143.7 (s, *C*-Me), 137.1 (s, ipsoAr), 128.9 (s, Ar), 125.7 (s, Ar), 125.6 (s, Ar), 124.1 (s, Ar), 100.7 (s, CH), 54.9 (s, C-Me), 25.3 (s, Me), 23.9 (s, Me), 20.9 (s, Me). $^{19}F\{^1H\}$ NMR: −78.8 (s, CF_3). Anal. Calcd for $C_{26}H_{26}F_3N_4O_5RhS$: C, 46.85; H, 3.93; N, 8.40. Found: C, 47.04; H, 4.01; N, 8.55.

[Rh(tmtaaH$_2$)(COD)][OTf] (7). To a solution of **1** (0.105 g, 0.19 mmol) in THF was added HOTf (0.017 mL, 0.19 mmol). The solution was stirred for 1 h at room temperature, and then the solvent was partially removed under vacuum and the solution was cooled to −30 °C to yield yellow plates, which were identified as **7**·1/2THF (0.086 g, 64%). ^1H NMR ($CDCl_3$, rt): δ 12.32 (s, 1 H, NH), 7.15 (m, 6 H, Ar), 6.75 (m, 2 H, Ar), 4.88 (s, 1 H), 4.82 (d, $^2J_{H-H}$ = 15.11 Hz, 1 H), 4.23 (d, $^2J_{H-H}$ = 15.11 Hz, 1 H), 4.36 (m, 2 H, COD), 3.73 (m, 2 H, THF), 2.91 (m, 2 H, COD), 2.54 (m, 2 H, COD), 2.12 (s, 6 H, Me), 2.02 (m, 2 H, COD), 1.99 (s, 6 H, Me), 1.87 (m, 2 H, COD), 1.83 (m, 2 H, THF), 1.60 (m, 2 H, COD). $^{13}C\{^1H\}$ NMR: δ 179.2 (s, ipsoAr), 160.8 (s, *C*-Me), 140.2 (s, *C*-Me), 136.9 (s, ipsoAr), 127.7 (s, Ar), 125.3 (s, Ar), 125.1 (s, Ar), 121.3 (s, Ar), 100.6 (s, CH), 87.2 (d, $^1J_{Rh-C}$ = 12.2 Hz, COD), 85.8 (d, $^1J_{Rh-C}$ = 12.2 Hz, COD), 68.6 (s, THF), 51.6 (s, CH), 30.9 (COD), 30.6 (s, COD), 26.3 (s, THF), 25.7 (s, Me), 21.5 (s, Me). $^{19}F\{^1H\}$ NMR: δ −78.6 (s, CF_3). Anal. Calcd for $C_{33}H_{40}F_3N_4O_{3.5}RhS$: C, 53.51; H, 5.48; N, 7.56. Found: C, 53.39; H, 5.51; N, 7.36.

[Rh(tmtaaH$_2$)(CO)$_2$][OTf] (8). To a solution of **3** (0.110 g, 0.22 mmol) in CH_2Cl_2 at −30 °C was added HOTf (0.019 mL, 0.22 mmol). The solution was stirred for 30 min, and then the solvent was removed under vacuum. The residue was extracted with THF, and the solution was cooled to −30 °C during 24 h to yield complex **8** as a yellow crystalline solid (0.074 g, 52%). IR (ν C−O): 2097 (vs), 2024 (vs). ^1H NMR ($CDCl_3$, rt): δ 12.69 (s, 1 H, NH), 7.12 (m, 6 H, Ar), 7.11 (m, 2 H, Ar), 4.89 (s, 1 H), 4.64 (d, $^2J_{H-H}$ = 15.98 Hz, 1 H), 4.43 (d, $^2J_{H-H}$ = 15.98 Hz, 1 H), 2.20 (s, 6 H, Me), 2.02 (s, 6 H, Me). $^{13}C\{^1H\}$ NMR: δ 184.4 (s, ipsoAr), 182.5 (d, $^1J_{Rh-C}$ = 72.1 Hz, CO), 161.3 (s, *C*-Me), 143.5 (s, *C*-Me), 136.6 (s, ipsoAr), 128.6 (s, Ar), 125.9 (s, Ar), 125.2 (s, Ar), 122.2 (s, Ar), 100.6 (s, CH), 51.5 (s, CH), 25.1 (s, Me), 21.0 (s, Me). $^{19}F\{^1H\}$ NMR: δ −78.5 (s, CF_3). Anal. Calcd for $C_{25}H_{24}F_3N_4O_5RhS$: C, 46.02; H, 3.71; N, 8.58. Found: C, 46.12; H, 3.74; N, 8.76.

[Rh(CO)$_2$(tmtaa)Li(thf)] (9). To solution of [Rh(tmtaaH)(CO)$_2$] (0.059 g, 0.12 mmol) in THF was added a solution of $LiNTMS_2$·Et_2O (0.028 g, 0.12 mmol) in THF. The solution was stirred at room temperature for 1 h. After this time pentane was added and the mixture was cooled to −23 °C for 24 h to yield red crystals of the complex (0.050 g, 73%). IR (ν C−O): 2071 (vs), 2013 (vs). ^1H NMR (C_6D_6, rt): δ 1.06 (m, 4 H, THF), 1.68 (s, 6 H, Me), 1.86 (s, 6 H, Me), 3.29 (m, 4 H, THF), 4.59 (s, 1 H, CH), 4.86 (s, 1 H, CH), 6.84 (m, 2 H, Ar), 6.99 (m, 4 H, Ar), 7.11 (m, 2 H, Ar). $^{13}C\{^1H\}$ NMR: δ 186.5 (d, $^1J_{Rh-C}$ = 65.1 Hz, CO), 160.2 (s, *C*-Me), 159.8 (s, *C*-Me), 150.4 (s, ipsoAr), 125.6 (s, Ar), 124.8 (s, Ar), 123.6 (s, Ar), 121.1 (s, Ar), 99.4 (s, CH), 95.7 (s, CH), 67.9 (s, THF), 25.1 (s, THF), 22.1 (s, Me), 21.4 (s, Me). Anal. Calcd for $C_{28}H_{30}N_4O_3RhLi$: C, 57.94; H, 5.21; N, 9.65. Found: C, 54.78; H, 4.53; N, 8.84.

[Ir(CO)$_2$(tmtaa)Li(thf)] (10). To a solution of [Ir(tmtaaH)(CO)$_2$] (0.084 g, 0.14 mmol) in THF was added a solution of $LiNTMS_2$·Et_2O (0.034 g, 0.14 mmol) in THF. The solution was stirred at room temperature for 1 h. After this time pentane was added and the mixture was cooled to −23 °C for 24 h to yield red crystals of the complex (0.061 g, 64%). IR (ν C−O): 2039 (vs), 1981 (vs). ^1H NMR (C_6D_6, rt): δ 1.07 (m, 4 H, THF), 1.62 (s, 6 H, Me), 1.83 (s, 6 H, Me), 3.30 (m, 4 H, THF), 4.55 (s, 1 H, CH), 4.88 (s, 1 H, CH), 6.88 (m, 2 H, Ar), 6.98 (m, 4 H, Ar), 7.06 (m, 2 H, Ar). $^{13}C\{^1H\}$ NMR: δ 176.5 (s, CO), 160.5 (s, *C*-Me), 159.8 (s, *C*-Me), 150.5 (s, ipsoAr), 149.4 (s, ipsoAr), 126.2 (s, Ar), 124.7 (s, Ar), 123.4 (s, Ar), 120.7 (s, Ar), 101.6 (s, CH), 95.6 (s, CH), 67.9 (s, THF), 25.1 (s, THF), 22.2 (s, Me), 21.2 (s, Me). Anal. Calcd for $C_{28}H_{30}N_4O_3IrLi$: C, 50.21; H, 4.51; N, 8.36. Found: C, 50.07; H, 4.27; N, 8.26.

[Rh(tmtaaMe)(CO)$_2$] (11). To solution of **9** (0.050 g, 0.086 mmol) in THF at −20 °C was added MeI (0.012 g, 0.086 mmol). The solution was stirred for 10 min, and then the solvent was removed under vacuum. The residue was extracted with pentane, and the solution was cooled to −20 °C during 14 h to yield red crystals of complex **11**·1/2pentane (0.021 g, 47%). The pentane that crystallizes with **11** was observed in the NMR spectra. IR (ν C−O): 2052 (vs), 1985 (vs). ^1H NMR (C_6D_6, rt): δ 1.12 (d, $^3J_{H-H}$ = 7.3 Hz, 3 H, Me), 1.74 (s, 6 H, Me), 1.76 (s, 6 H, Me), 3.28 (q, $^3J_{H-H}$ = 7.3 Hz, 1 H, C−H), 4.86 (s, 1 H, CH), 6.57 (m, 2 H, Ar), 6.88 (m, 4 H, Ar), 6.97 (m, 2 H, Ar). ^1H NMR (C_7D_8, 193 K): 1.09 (br, 3 H, Me), 1.18 (br, 3 H, Me), 1.61 (br, 3 H, Me), 1.81 (br, 3 H, Me), 2.22 (br, 3 H, Me), 3.25 (br, 1 H, CH), 4.79 (s, 1 H, CH), 6.50 (br, 2 H, Ar), 6.83 (br, 6 H, Ar). $^{13}C\{^1H\}$ NMR: δ 186.4 (d, $^1J_{Rh-C}$ = 66.7 Hz, CO), 172.9 (s, *C*-Me), 159.4 (s, *C*-Me), 146.7 (s, ipsoAr), 146.5 (s, ipsoAr), 125.7 (s, Ar), 124.4 (s, Ar), 123.0 (s, Ar), 119.5 (s, Ar), 99.3 (d, J_{Rh-C} = 2.7 Hz, CH), 54.5 (s, CH), 22.4 (s, Me), 20.2 (s, Me), 15.8 (s, Me). Anal. Calcd for $C_{27.5}H_{31}N_4O_2Rh$: C, 59.78; H, 5.65; N, 10.14. Found: C, 59.57; H, 5.52; N, 10.25.

[Ir(tmtaaMe)(CO)$_2$] (12). To solution of [Ir(CO)$_2$(tmtaa)Li(thf)] (0.055 g, 0.082 mmol) in THF at −20 °C was added MeI (0.011 g, 0.082 mmol). The solution was stirred for 10 min, and then the solvent was removed under vacuum. The residue was extracted with pentane, and the resulting solution was cooled to −20 °C during 24 h to yield a yellow solid that was characterized as complex **12** (0.030 g, 60%). ^1H NMR (C_6D_6, rt): δ 1.07 (d, $^3J_{H-H}$ = 7.3 Hz, 3 H, Me), 1.69 (s, 6 H, Me), 1.71 (s, 6 H, Me), 3.22 (q, $^3J_{H-H}$ = 7.3 Hz, 1 H, C−H), 4.93 (s, 1 H, CH), 6.54 (m, 2 H, Ar), 6.88 (m, 4 H, Ar), 6.97 (m, 2 H, Ar). $^{13}C\{^1H\}$ NMR: δ 176.2 (s, CO), 173.2 (s, *C*-Me), 159.6 (s, *C*-Me), 146.7 (s, ipsoAr), 145.6 (s, ipsoAr), 126.5 (s, Ar), 124.1 (s, Ar), 122.8 (s, Ar), 119.3 (s, Ar), 101.6 (s, CH), 54.6 (s, CH), 22.5 (s, Me), 20.1 (s, Me), 15.7 (s, Me). This compound was not obtained analytically pure, as it was always contaminated by variable amounts of **4**.

[Rh(tmtaaMe)(CO)$_2$] (13). To solution of **6** (0.068 g, 0.10 mmol) in THF was added $LiNTMS_2$·Et_2O (0.024 g, 0.10 mmol), and the mixture was stirred at room temperature for 1 h. The solvent was removed under vacuum and the residue extracted with CH_2Cl_2. The solvent was evaporated, the residue was extracted with THF, and the solution was cooled to −30 °C for 1 day to yield the complex as dark yellow crystals (0.031 g, 59%). IR (ν C−O): 2055 (vs), 1992 (vs). ^1H NMR ($CDCl_3$, rt): δ 1.69 (s, 6 H, Me), 1.81 (s, 3 H, Me), 1.89 (s, 6 H, Me), 4.61 (s, 1 H, CH), 6.89 (m, 2 H, Ar),

6.99 (m, 4 H, Ar), 7.14 (m, 2 H, Ar), 12.37 (s, 1 H, NH). $^{13}C\{^1H\}$ NMR: δ 186.4 (d, $^1J_{Rh-C} = 67.1$ Hz, CO), 159.6 (s, *C*-Me), 158.7 (s, *C*-Me), 148.8 (s, ipsoAr), 141.4 (s, ipsoAr), 125.5 (s, Ar), 124.6 (s, Ar), 123.9 (s, Ar), 123.6 (s, Ar), 99.8 (s, CH), 21.1 (s, Me), 18.9 (s, Me), 18.4 (s, Me). Anal. Calcd for $C_{25}H_{25}N_4O_2Rh$: C, 58.15; H, 4.88; N, 10.85. Found: C, 57.87; H, 4.90; N, 10.77.

[Rh(CO)$_2$(tmtaa)Rh(COD)] (14). A mixture of **3** (0.101 g, 0.20 mmol) and [Rh$_2$(COD)$_2$(μ-OH)$_2$] (0.046 g, 0.10 mmol) in toluene was heated at 85 °C for 3 h. After cooling to room temperature the solvent was removed under vacuum and the residue washed with pentane to yield the dimetallic derivative as dark red crystals (0.104 g, 72%). IR (ν C−O): 2050 (vs), 1980 (vs). ^1H NMR (C_6D_6, rt): δ 1.27 (m, 2 H, COD), 1.46 (s, 6 H, Me), 1.54 (s, 6 H, Me), 1.60 (m, 2 H, COD), 2.23 (m, 2 H, COD), 2.32 (m, 2 H, COD), 2.89 (m, 2 H, COD), 4.43 (m, 2 H, COD), 4.56 (s, 1 H, CH), 4.63 (s, 1 H, CH), 6.87 (m, 6 H, Ar), 7.00 (m, 2 H, Ar). $^{13}C\{^1H\}$ NMR: δ 188.1 (d, $^1J_{Rh-C} = 66.7$ Hz, CO), 158.6 (s, *C*-Me), 158.0 (s, *C*-Me), 150.3 (s, ipsoAr), 148.4 (s, ipsoAr), 125.7 (s, Ar), 124.4 (s, Ar), 124.3 (s, Ar), 124.2 (s, Ar), 99.4 (s, CH), 99.2 (s, CH), 78.5 (d, $^1J_{C-H} = 12.9$ Hz, COD), 75.3 (d, $^1J_{C-H} = 12.6$ Hz, COD), 31.0 (COD), 30.2 (s, COD), 22.5 (s, Me), 21.2 (s, Me). Anal. Calcd for $C_{32}H_{34}N_4O_2Rh_2$: C, 53.95; H, 4.81; N, 7.86. Found: C, 54.10; H, 4.96; N, 7.85.

[Rh$_2$(tmtaa)(CO)$_4$] (15). A solution of **14** (0.050 g, 0.070 mmol) in toluene was heated at 80 °C under CO atmosphere for 9 h. After that the solution was cooled to room temperature, forming red crystals of **15** (yield 0.033 g, 71%). ^1H NMR ($CDCl_3$, rt): δ 1.74 (12 H, Me), 4.69 (s, 2 H, CH), 7.26 (m, 8 H, Ar).

[Ir(CO)$_2$(tmtaa)Rh(COD)] (16). A mixture of **4** (0.093 g, 0.16 mmol) and [Rh$_2$(COD)$_2$(μ-OH)$_2$] (0.036 g, 0.08 mmol) in toluene was heated at 85 °C for 3 h. Cooling the solution to −23 °C for 15 h yielded red crystals of the dark red heterometallic complex (0.078 g, 62%). IR (ν C−O): 2032 (vs), 1957 (vs). ^1H NMR (C_6D_6, rt): δ 1.28 (m, 2 H, COD), 1.45 (s, 6 H, Me), 1.46 (s, 6 H, Me), 1.67 (m, 2 H, COD), 2.31 (m, 4 H, COD), 2.87 (m, 2 H, COD), 4.40 (m, 2 H, COD), 4.52 (s, 1 H, CH), 4.77 (s, 1 H, CH), 6.74 (m, 2 H, Ar), 6.88 (m, 6 H, Ar). $^{13}C\{^1H\}$ NMR: δ 177.6 (s, CO), 159.0 (s, *C*-Me), 158.2 (s, *C*-Me), 149.7 (s, ipsoAr), 148.5 (s, ipsoAr), 125.4 (s, Ar), 124.9 (s, Ar), 124.0 (s, Ar), 123.7 (s, Ar), 100.9 (s, CH), 99.4 (s, CH), 78.5 (d, $^1J_{Rh-C} = 13.3$ Hz, COD), 74.4 (d, $^1J_{Rh-C} = 12.6$ Hz, COD), 31.1 (COD), 30.0 (s, COD), 22.3 (s, Me), 21.2 (s, Me). Anal. Calcd for $C_{32}H_{34}N_4O_2IrRh$: C, 47.93; H, 4.27; N, 6.99. Found: C, 47.91; H, 4.46; N, 6.88.

[Ir(CO)$_2$(tmtaa)Rh(CO)$_2$] (17). A solution of [Ir(CO)$_2$(tmtaa)-Rh(COD)] (0.045 g, 0.056 mmol) in toluene was stirred at 70 °C under CO atmosphere during 6 h. After that the solution was cooled to −30 °C to yield purple crystals of **17** (yield 0.026 g, 65%). IR (ν C−O): 2056 (vs), 2040 (m), 2001 (s), 1984 (m). ^1H NMR ($CDCl_3$, rt): δ 1.76 (12 H, Me), 4.65 (s, 1 H, CH), 4.80 (s, 1 H, CH), 7.26 (m, 8 H, Ar). $^{13}C\{^1H\}$ NMR: δ 186.5 (d, $^1J_{Rh-C} = 67.2$ Hz, CO), 175.1 (s, CO), 160.4 (s, *C*-Me), 151.5 (s, ipsoAr), 151.1 (s, ipsoAr), 126.8 (s, Ar), 125.7 (s, Ar), 125.0 (s, Ar), 124.6 (s, Ar), 101.6 (s, CH), 99.6 (s, CH), 22.1 (s, Me), 21.9 (s, Me). Anal. Calcd for $C_{26}H_{22}N_4O_4IrRh$: C, 41.66; H, 2.95; N, 7.47. Found: C, 41.61; H, 2.92; N, 7.49.

Crystallographic Studies. A crystal of appropriate dimensions was mounted on a glass fiber using Paratone N hydrocarbon oil. All measurements were made on a Bruker SMART 1K CCD diffractometer.[29] Cell constants and an orientation matrix were obtained for the measured positions of reflections with $I > 10\sigma$ to give the unit cell. The systematic absences uniquely determined the space group in each case. An arbitrary hemisphere of data was collected at low temperature (see Table 1) using the ω scan technique with 0.3° scans counted for 10 s per frame. Data were integrated using SAINT[30] and corrected for Lorentz and polarization effects. The data were analyzed for agreement and absorption using XPREP,[31] and an empirical absorption correction based on comparison of redundant and equivalent reflections was applied using SADABS.[32] The structures were solved by direct methods and expanded using Fourier techniques. Non-hydrogen atoms were refined anisotropically, and the hydrogen atoms were included in calculated positions, but not refined (unless stated otherwise). The structures were solved and refined using the software packages SHELXS-97 (structure solution)[33] and SHELXL-97 (refinement).[34]

Crystallographic data are deposited with Cambridge Crystallographic Data Centre. Copies of the data (CCDC 294896, 294897, 604679, and 604680) can be obtained free of charge via http://www.ccdc.cam.ac.uk/data_request/cif by e-mailing data_request@ccdc.cam.ac.uk or by contacting The Cambridge Crystallographic Data Centre, 12 Union Road, Cambridge CB 1EZ, UK; fax +44 1223 336033.

Acknowledgment. This work was supported by the Director Office of Energy Research, Office of Basic Energy Sciences Division of the U.S. Department of Energy under Contract No. DE-AC03-76SF00098. R.F. thanks Spanish Ministry of Educación, Cultura y Deporte for a Sabbatical Fellowship. We thank Dr. F. J. Hollander and Dr. A. Oliver at the CHEXRAY facility at UC Berkeley for their help with the X-ray crystallographic studies and Dr. P. Terreros for her help with the IR spectra. The authors wish to thank a referee for helpful comments on the original manuscript. These comments lead us to do crystal structures of complexes **6** and **11** that resulted in changes in their stereochemistry from those in the original manuscript.

Supporting Information Available: Crystallographic data, labeling diagrams, tables giving atomic positions, anisotropic thermal parameters, bond distances, bond angles, torsion angles, and least-squares planes. This material is available free of charge via the Internet at http://pubs.acs.org. Structure factor tables are available from the authors.

OM060039Y

(29) *SMART Area-Detector Software Package*; Bruker Analytical X-ray Systems, Inc.: Madison, WI, 2001−03.

(30) *SAINT SAX Area-Dectector Integration Program*, 5.04 ed.; Siemens Industrial Automation, Inc.: Madison, WI, 2003.

(31) Sheldrick, G. M. *XPREP*, 6.12 ed.; Siemens Industrial Automation, Inc.: Madison, WI, 2001.

(32) Sheldrick, G. M. *SADABS*, 2.05 ed.; Bruker Analytical X-ray Systems, Inc.: Madison, WI, 2003.

(33) Sheldrick, G. M. *SHELXS-97*; University of Göttingen: Germany, 1997.

(34) Sheldrick, G. M. *SHELXL-97*; University of Göttingen: Germany, 1997.